Regular paper

Journal of the KIECS. pp. 59-70, vol. 17, no. 1, Feb. 28. 2022, t. 111, pISSN 1975-8170 | eISSN 2288-2189
http://dx.doi.org/10.13067/JKIECS.2022.17.1.59

다중 슬라이딩 표면 제어 기법에 기반한 쿼드로터의 능동 결함 허용 제어

황남웅* · 김병수**

Active Fault Tolerant Control of Quadrotor Based on Multiple Sliding Surface Control Method

Nam-Eung Hwang* · Byung-Soo Kim**

요약

본 논문에서는 쿼드로터의 모터 하나가 완전히 고장이 발생한 경우 쿼드로터의 위치 제어를 위한 능동 결함 허용 제어 방법을 제안한다. 소각의 가정 없이 라그랑지 방정식을 사용하여 쿼드로터의 동적 방정식을 구한다. 제안한 방법에서는 모터의 결함 검출을 위해 고장 검출 및 진단(FDD) 모듈과 고장 검출 및 분리(FDI) 모듈로 구성되는 고장 검출 모듈을 설계한다. FDD 모듈에서는 구해진 동력학에 기반하여 쿼드로터의 상태를 관측하는 비선형 관측기를 설계한다. 관측된 쿼드로터의 상태들을 이용하여, 유수 신호를 설계하고 결함을 검출하기 위한 유수 신호의 적절한 문턱 값을 설정한다. 또한 설계된 추가 조건을 사용하여 결함 위치를 알아내기 위한 FDI 모듈을 설계한다. 모터의 결함을 검출한 후 쿼드로터가 원하는 경로로 비행하기 위해 다중 슬라이딩 표면 제어 기법에 기반한 결함 허용 제어기를 설계한다. 마지막으로, 모의실험을 통해 제안한 능동 결함 허용 제어 방법이 효용성을 검증한다.

ABSTRACT

In this paper, we proposed an active fault tolerant control (AFTC) method for the position control of a quadrotor with complete loss of effectiveness of one motor. We obtained the dynamics of a quadrotor using Lagrangian equation without small angle assumption. For detecting the fault on a motor, we designed a fault detection module, which consists of the fault detection and diagnosis (FDD) module and the fault detection and isolation (FDI) module. For the FDD module, we designed a nonlinear observer that observes the states of a quadrotor based on the obtained dynamics. Using the observed states of a quadrotor, we designed residual signals and set the appropriate threshold values of residual signals to detect the fault. Also, we designed an FDI module to identify the fault location using the designed additional conditions. To make a quadrotor track the desired path after detecting the fault of a motor, we designed a fault tolerant controller based on the multiple sliding surface control (MSSC) technique. Finally, through simulations, we verified the effectiveness of the proposed AFTC method for a quadrotor with complete loss of effectiveness of one motor.

키워드

Active Fault Tolerant Control, Fault Tolerant Control, Fault Diagnosis and Isolation, Multiple Sliding Surface Control, Nonlinear Control, Robust Control.
능동 결함 허용 제어, 결함 허용 제어, 장애 진단 및 격리, 다중 슬라이딩 표면 제어, 비선형 제어, 강력 제어

* 한화시스템 미래정보통신연구소 지상전투체계팀 (skadnd144@hanwha.com)
** 교신저자 : 경기대학교 대학원 전자공학과
· 접 수 일 : 2021. 10. 25
· 수정완료일 : 2021. 12. 21
· 게재확정일 : 2022. 02. 17
· Received : Oct. 25, 2021, Revised : Dec. 21, 2021, Accepted : Feb. 17, 2022
· Corresponding Author : Byung-Soo Kim
Department of Electonic Engineering, Kyonggi University
Email : 20131102133@kyonggi.ac.kr

I. INTRODUCTION

A multirotor is one of small unmanned aerial vehicles (UAVs). Since a multirotor has the structural symmetry, it can do the vertical take-off and landing (VTOL) and can be easily manufactured. Because of these advantages of a multi- rotor, it is among the more commonly used types of UAV. However, due to poor control and unexpected accident, a multirotor might have some faults on sensors or motors, thus the collision accidents of multirotor usually happen. To prevent that, the fault tolerant control of a multirotor is a key topic nowadays. When the sensor faults occur on a multirotor, the sensing data is compensated by filters to control a multirotor. However, when the faults occur on motors of a multirotor, control strategy should be changed to control a multirotor. In [1-4], passive fault tolerant control (PFTC) is suggested for a multirotor UAV with the fault on motors. However, PFTC is useful in the case of only partial loss of effectiveness on motors because it does not have the fault detection module and only depends on the robustness of controller. In [2-9], active fault tolerant control (AFTC) is designed for the fault on motors of a multirotor. AFTC has better performance than PFTC because it has fault detection module and controllers for healthy and faulty conditions seperately. In [2] and [8], AFTC is designed using the well-known control strategies. They also applied the designed controller to a real quadrotor. However, they did not address the fault detection module and assumed that the time between the occurrence of a fault and the detection of a fault, that is, decision making time is 0s. In [3-7] and [9], they designed an AFTC and tested it with the fault detection modules. However, the fault detection modules that are used in these paper only detects whether the fault occurs or not. In other words, they cannot know where the fault occurs. In [4] and [7], they designed an AFTC of a quadrotor with coaxial propeller system and octorotor which have 8 motors on a multirotor. These systems that have more actuators than state variables are called overactuated system. These systems are easy to design a fault tolerant controller because they have 2 motors more than state variables. However, a quadrotor system is an underactuated system since it has more state variables than actuators. In other words, it does not have extra motors to control state variables, so it is difficult to design a fault tolerant controller when the fault occurs on motors. In [1-4] and [9], they assumed that a multirotor has the fault with partial loss of effectiveness of motors. It is possible to control a multirotor safely with partial loss of effectiveness of motors. However, when a multirotor has the fault with complete loss of effectiveness of motors, it is difficult to control a multirotor safely. Thus in [8], only attitudes and altitude, not position are controlled to land a multirotor safely using a PID control strategy.

In this paper, we propose an AFTC method for the position control of a quadrotor with complete loss of effectiveness of one motor. We obtain the dynamics of a quadrotor using Lagrangian equation without small angle assumption. In the proposed method, we design a nonlinear observer that observes the state variables of a quadrotor to make the residual signals. Using the states of a quadrotor and the state variables observed by the designed nonlinear observer, we design residual signals for the fault detection and diagnosis (FDD) module and the fault detection and isolation (FDI) module. We set some threshold values and conditions of residual signals to detect the fault occurrence and the fault location. Also we design a fault tolerant controller for tracking the desired path after occurring fault, which is based on the multiple sliding surface control (MSSC) technique. Finally, we demonstrate the effectiveness of the proposed AFTC via simulation results.

II. MODELING OF QUADROTOR

A quadrotor has 4 motors with propellers symmetrically. To prevent spinning, two motors facing each other on a quadrotor turn clockwise, on the other hand, the others turn counter-clockwise. A quadrotor used in this paper is shown in Fig. 1, where ohm_1, ohm_2, ohm_3 and ohm_4 the speed of each motor

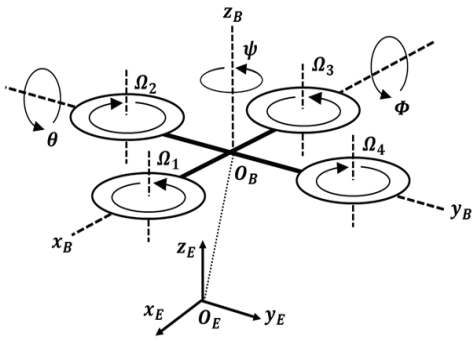

Fig. 1. The quadrotor system

To derive the model of a quadrotor, two frames are used: one is the body-fixed frame and the other is the earth-inertia frame [10]. The body-fixed frame is described on a quadrotor with origin at the center of mass of a quadrotor, which is represented as follow:

$$\{\zeta_B\} = (x_B, y_B, z_B) \tag{1}$$

The translational and rotational velocities of a quadrotor on each axis are used as the state variables in the body-fixed frame as follows:

$$\xi^B = (u, v, w, p, q, r) \tag{2}$$

where (u,v,w) is the translational velocity of a quadrotor on each axis and (p,q,r) is the rotational velocity of a quadrotor on each axis. The earth-inertia frame is described on the earth with origin at the center of earth, which is represented as

$$\{\zeta_E\} = (x_E, y_E, z_E) \tag{3}$$

The position and angles of a quadrotor on each axis are used as the state variables in the earth-inertia frame as follows:

$$\xi^E = (x, y, z, \phi, \theta, \psi) \tag{4}$$

where (x,y,z) is the position of a quadrotor on each axis and (ϕ,θ,ψ) is the angles of a quadrotor on each axis. For modeling a quadrotor, we set Lagrangian function as follows:

$$L = K - P \tag{5}$$

where K and P are the kinetic and potential energies of a quadrotor, respectively. The dynamics of a quadrotor can be obtained using the following Lagrangian equation:

$$\frac{d}{dt}\left(\frac{\partial L}{\partial \xi^B}\right) - \frac{\partial L}{\partial \xi^B} = \tau \tag{6}$$

where τ is the control input of a quadrotor. Then we can obtain the dynamics of a quadrotor expressed on the body-fixed frame as follows:

$$\begin{bmatrix} m_{3\times3} & 0_{3\times3} \\ 0_{3\times3} & I_{3\times3} \end{bmatrix} \begin{bmatrix} \dot{V}_B \\ \dot{\omega}_B \end{bmatrix} + \begin{bmatrix} \omega_B \times (m\, V_B) \\ \omega_B \times (I_{3\times3})\omega_B \end{bmatrix} = \begin{bmatrix} F_B \\ \tau_B \end{bmatrix} \tag{7}$$

where $m_{3\times3}$ denotes a 3×3 diagonal matrix with the mass of a quadrotor, $I_{3\times3}$ denotes a 3×3 diagonal matrix with the moments of inertia I_x, I_y, I_z that are on each axis on the body-fixed frame, and F_B, τ_B are the control inputs of a quadrotor for the translational and rotational movements, respectively. The dynamics of a quadrotor can be described as follows [11-13]:

$$
\begin{aligned}
\dot{u} &= (vr - wq) + gS_{\theta}, \\
\dot{v} &= (wq - ur) - gC_{\theta}S_{\phi}, \\
\dot{w} &= (uq - v[) - gC_{\theta}C_{\phi} + \frac{u_1}{m}, \\
\dot{p} &= \frac{I_y - I_z}{I_x}qr - \frac{J_{tp}}{I_x}qohm + \frac{U_2}{I_x}, \\
\dot{q} &= \frac{I_z - I_x}{I_y}pr + \frac{J_{tp}}{I_y}pohm + \frac{u_3}{I_y}, \\
\dot{r} &= \frac{I_x - I_y}{I_z}pq + \frac{u_4}{I_z},
\end{aligned} \tag{8}
$$

where g is the acceleration of gravity, u_1, u_2, u_3, u_4 are control inputs of a quadrotor, J_{tp} is the total moment of inertia of motor and propeller on each center of propeller, and $ohm$is the total rotational speed of motors described as the following form:

$$
ohm = ohm_1 - ohm_2 + ohm_3 - ohm_4 \tag{9}
$$

The dynamics of a quadrotor are more conveniently formulated in the body-fixed frame. However the dynamics of a quadrotor described on the body-fixed frame should be converted to those described on the earth-inertia frame for tracking control. The relation of the translational and rotational velocities between the body-fixed frame and the earth-inertia frame are described as follows [10]:

$$
V_E = (\dot{x}, \dot{y}, \dot{z}) = \dot{R}(u, v, w) = RV_B, \tag{10}
$$

$$
\omega_E = (\dot{\phi}, \dot{\theta}, \dot{\psi}) = W(p, q, r) = W\omega_B, \tag{11}
$$

where V_E, V_B are the translational velocity on the earth-inertia frame and the body-fixed frame, respectively, ω_E, ω_B are the rotational velocity on the earth-inertia frame and the body-fixed frame, respectively, and R and W are the rotation and translation matrices, respectively. The rotation and translation matrices R and W are expressed as

$$
R = \begin{bmatrix}
C_{\theta}C_{\psi} & S_{\phi}S_{\theta}C_{\psi} - C_{\phi}S_{\psi} & C_{\phi}S_{\theta}C_{\psi} + S_{\phi}S_{\psi} \\
C_{\theta}S_{\psi} & S_{\phi}S_{\theta}S_{\psi} + C_{\phi}C_{\psi} & C_{\phi}S_{\theta}S_{\psi} - S_{\phi}C_{\psi} \\
-S_{\theta} & S_{\phi}C_{\theta} & C_{\phi}C_{\theta}
\end{bmatrix}, \tag{12}
$$

$$
W = \begin{bmatrix}
1 & S_{\phi}T_{\theta} & C_{\phi}T_{\theta} \\
0 & C_{\phi} & -S_{\phi} \\
0 & \frac{S_{\phi}}{C_{\theta}} & \frac{C_{\phi}}{C_{\theta}}
\end{bmatrix}, \tag{13}
$$

where $S_{(\bullet)}, C_{(\bullet)}$, and $T_{(\bullet)}$ mean $\sin(\bullet)$, $\cos(\bullet)$, and $\tan(\bullet)$, respectively. The dynamics of a quadrotor described on the earth-inertia frame can be obtained with (8), (10), and (11). The control inputs of a quadrotor shown in Fig. 1 are expressed as the following form:

$$
\begin{aligned}
u_1 &= b(ohm_1^2 + ohm_2^2 + ohm_3^2 + ohm_4^2), \\
u_2 &= bl(ohm_4^2 - ohm_2^2), \\
u_3 &= bl(ohm_3^2 - ohm_1^2), \\
u_4 &= d(-ohm_1^2 + ohm_2^2 - ohm_3^2 + ohm_4^2),
\end{aligned} \tag{14}
$$

where b is the thrust factor of propeller, l is the distance between the center of a quadrotor and the center of each motor, and d is the drag factor of a quadrotor. The speed of each motor in this paper can be calculated as follows [14]:

$$
\dot{ohm}_i = K_m(ohm_i^{des} - ohm_i), \tag{15}
$$

where K_m is the motor coefficient and $ohm_i^{des}$is the desired speed of each motor for $i = 1, 2, \cdots, 4$. A quadrotor used in this paper is Asctec Hummingbird, where its parameters and limitations are listed in Tables 1 and 2, respectively.

Table 1. The parameters of Asctec Hummingbird.

Para-meter	Description	Value
m	Mass of quadrotor	$0.5[kg]$
I_x	Moment of inertia about x_B axis	2.3×10^{-3} $[kg \cdot m^2]$
I_y	Moment of inertia about y_B axis	2.3×10^{-3} $[kg \cdot m^2]$
I_z	Moment of inertia about z_B axis	5.09×10^{-3} $[kg \cdot m^2]$
l	Distance between center of the quadrotor to center of each propeller	$0.17[m]$
b	Thrust factor	1.83×10^{-4} $[N \cdot m^2]$
d	Drag factor	0.052 $[N \cdot m \cdot S^2$
J_{tp}	Total moment of inertia of motor and propeller about center of each motor axis	6.5×10^{-5} $[kg \cdot m^2]$
g	Acceleration of graviry	9.806 $[kg \cdot m/s^2]$
K_m	Motor coefficient	$20[s^{-1}]$

Table 2. The limitations of Asctec Hummingbird in non-faulty case

Limitations	Description
$-\pi/6<\phi<\pi/6[rad]$	Limitation of angle ϕ
$-\pi/6<\theta<\pi/6[rad]$	Limitation of angle θ
$-\pi<\psi<\pi[rad]$	Limitation of angle ψ
$\dot{x}<16[m/s]$	Limitation of translational velocity about x axis
$\dot{y}<16[m/s]$	Limitation of translational velocity about y axis
$\dot{z}<8[m/s]$	Limitation of translational velocity about z axis
$-\pi/6<\dot{\phi}<\pi/6[rad/s]$	Limitation of rotational velocity about ϕ
$-\pi/6<\dot{\theta}<\pi/6[rad/s]$	Limitation of rotational velocity about θ
$-5\pi/3<\dot{\psi}<5\pi/3[rad/$	Limitation of rotational velocity about ψ

III. DESIGN OF ACTIVE FAULT TOLERANT CONTROLLER

In this section, we design an active fault tolerant controller of a quadrotor with complete loss of effectiveness of one motor. The proposed active fault tolerant controller is designed with three steps: the fault detection, the fault isolation, and the switching to active fault tolerant controller.

3.1 Design of Fault Detection Module

To detect the fault occurring on a quadrotor, the FDD module and the FDI module should be designed. For this purpose, the nonlinear observer of a quadrotor is used. The dynamics of a quadrotor (8) can be described as follows:

$$\dot{\underline{x}} = \underline{f}(\underline{x}) + G(\underline{x})\underline{u}, \tag{16}$$

where

$$\underline{x} = (x,u,v,v,z,w,\phi,p,\theta,q,\psi,r),$$

$$\underline{f}(\underline{x}) = \begin{bmatrix} R(1,1)u + R(1,2)v + R(1,3)w \\ (vr - wq) + gS_\theta \\ R(2,1)u + R(2,2)v + R(2,3)w \\ (\wp - ur) - gC_\theta S_\phi \\ R(3,1)u + R(3,2)v + R(3,3)w \\ (uq - vp) - gC_\theta C_\phi \\ W(1,1)p + W(1,2)q + W(1,3)r \\ \dfrac{I_y - I_z}{I_x}qr - \dfrac{J_{tp}}{I_x}qohm \\ W(2,1)p + W(2,2)q + W(2,3)r \\ \dfrac{I_z - I_x}{I_y}pr - \dfrac{J_{tp}}{I_y}pohm \\ W(3,1)p + W(3,2)q + W(3,3)r \\ \dfrac{I_y - I_x}{I_x}pq \end{bmatrix},$$

$$G(\underline{x}) = \begin{bmatrix} 0 & 0 & 0 & 0 \\ 0 & 0 & 0 & 0 \\ 0 & 0 & 0 & 0 \\ 0 & 0 & 0 & 0 \\ 0 & 0 & 0 & 0 \\ 1/m & 0 & 0 & 0 \\ 0 & 0 & 0 & 0 \\ 0 & 1/I_x & 0 & 0 \\ 0 & 0 & 0 & 0 \\ 0 & 0 & 1/I_y & 0 \\ 0 & 0 & 0 & 0 \\ 0 & 0 & 0 & 1/I_z \end{bmatrix},$$

$\underline{u} = (u_1, u_2, u_3, u_4)$.

Similarly, we design a nonlinear observer as the following form [15]:

$$\dot{\underline{x}}_{ob} = \underline{f}(\underline{x}_{ob}) + \underline{G}(\underline{x}_{ob})\underline{u} + L(\underline{x} - \underline{x}_{ob}), \quad (17)$$

where $\underline{x}_{ob}$ is the observed states of a quadrotor through nonlinear observer and L is a 12×12 diagonal matrix.

Theorem 1: The observed states of a quadrotor asymptotically converges to the states of a quadrotor if a diagonal matrix L is set as follows:

$$L = \frac{\underline{f}(\underline{x}) - \underline{f}(\underline{x}_{ob}) + [G(\underline{x}) - \underline{G}(\underline{x}_{ob})]\underline{u}}{\underline{e}(i)} + \eta, \quad (18)$$

where $\underline{e}(i) = \underline{x}(i) - \underline{x}_{ob}(i)$ is the component of error vector and η is a positive constant.

Proof: we define the error vector as the following form:

$$\underline{e} = \underline{x} - \underline{x}_{ob} \quad (19)$$

Using (19), we choose the Lyapunov function candidate as

$$V_1 = \frac{1}{2}\underline{e}^T\underline{e} \quad (20)$$

The time derivative of (20) is calculated as

$$\begin{aligned} \dot{V}_1 &= \underline{\dot{e}}^T\underline{e} \\ &= [\underline{f}(\underline{x}) - \underline{f}(\underline{x}_{ob}) + G(\underline{x}) - G(\underline{x}_{ob})\underline{u} - L\underline{e}]^T\underline{e}. \end{aligned} \quad (21)$$

If we select a diagonal matrix L as (18), then (21) can be expressed as follows:

$$\dot{V}_1 = -\eta\underline{e}^T\underline{e} \quad (22)$$

Since the Lyapunov candidate (20) is positive definite and its time-derivative (22) is negative definite, the error vector (19) converges to 0 by Lyapunov theorem. It means the observed states of a quadrotor asymptotically converges to the states of a quadrotor.

The designed nonlinear observer observes the states of a quadrotor within the limitation as listed in Table 2. For detecting the fault on one motor, the residual signals are designed as the following form [16]:

$$r_1 = \phi - \phi_{ob},$$
$$r_2 = \theta - \theta_{ob}$$

When the fault occurs on one motor, a quadrotor will tilt to the ϕ or θ directions. However, the designed observer only observes the states of quadrotor within the limitation, so the residual signals will be larger. Therefore fault diagnosis and detection module is designed as follows:

$$\begin{array}{ll} \text{no fault} & -\sigma_\phi < \mathrm{r}_1 < \sigma_\phi \text{ and } -\sigma_\theta < r_1 < \sigma_\theta, \\ \text{fault} & \text{otherwise} \end{array}$$

where σ_ϕ and σ_θ are the threshold value of ϕ and θ, respectively. The smaller σ_ϕ and σ_θ are, the shorter the time between the fault occuring point and the controller switching point. However, it can be misrecognized in non-faulty case because of some noise. Thus, σ_ϕ and σ_θ should be set appropriately. To control a quadrotor with complete loss of effectiveness of one motor, not only

detecting the fault but also isolating the fault is needed. For this purpose, we design an FDI module. Without loss of generality, it is assumed that motor 1 in Fig. 1 has the fault. When motor 1 has the fault, the thrust force of motor 1 will be 0 thus a quadrotor with fault will be tilted to the positive θ direction. However, it will be tilted to the ϕ direction because of the Coriolis force. Thus the size of residual signals should be compared in order to isolate the fault. Finally, the conditions of residual signals for detection and isolation of the fault are described as follows:

$$\begin{array}{ll}\text{no fault} & -\sigma_\phi < r_1 < \sigma_\phi \text{ and } -\sigma_\theta < r_1 < \sigma_\theta,\\ \text{fault on motor 1} & \sigma_\theta < r_1 \text{ and } |r_2| < |r_1|,\\ \text{fault on motor 2} & \sigma_\phi < r_2 \text{ and } |r_1| < |r_2|,\\ \text{fault on motor 3} & r_1 < -\sigma_\theta \text{ and } |r_2| < |r_1|,\\ \text{fault on motor 4} & r_2 < -\sigma_\phi \text{ and } |r_1| < |r_2|.\end{array}$$

3.2 Design of Fault Tolerant Controller

After the diagnosis and isolation of fault, the fault accommodation is needed to control a quadrotor with complete loss of one motor. In fault accommodation step, the controller that is applied to a quadrotor before occurring the fault is switched to the fault tolerant controller. For the design of the fault tolerant controller of a quadrotor with complete loss of one motor, the dynamics of a quadrotor (8) is described as follows:

$$\begin{aligned} dotunderx_1 &= B_1(\underline{x}_1)\underline{x}_2\\ dotunderx_2 &= \underline{f}_2(\underline{x}_1,\underline{x}_2)+B_2(\underline{x}_1,\underline{x}_2)\underline{u}, \end{aligned} \tag{23}$$

where,

$$\begin{aligned} \underline{x}_1 &= (x,y,z,\phi,\theta,\psi),\\ \underline{x}_2 &= (u,v,w,q,p,r),\\ B_1(\underline{x}_1) &= \begin{bmatrix} R & 0_{3\times3}\\ 0_{3\times3} & W\end{bmatrix}, \end{aligned}$$

$$\underline{f}_2(\underline{x}_1,\underline{x}_2) = \begin{bmatrix} (vr-wq)+gS_\theta\\ (\wp-ur)-gC_\theta S_\phi\\ (uq-vp)-gC_\theta C_\phi\\ \dfrac{I_y-I_z}{I_x}qr-\dfrac{J_{tp}}{I_x}qohm\\ \dfrac{I_z-I_x}{I_y}+\dfrac{J_{tp}}{I_y}pohm\\ \dfrac{I_y-I_z}{I_x}pq \end{bmatrix},$$

$$B_2(\underline{x}_1,\underline{x}_2) = \begin{bmatrix} 0 & 0 & 0 & 0\\ 0 & 0 & 0 & 0\\ 1/m & 0 & 0 & 0\\ 0 & 1/I_x & 0 & 0\\ 0 & 0 & 1/I_y & 0\\ 0 & 0 & 0 & 1/I_z \end{bmatrix}.$$

To control a quadrotor described in (23), the sliding surfaces are set as follows:

$$\begin{aligned} \underline{s}_1 &= \underline{x}_1-\underline{x}_{1d},\\ \underline{s}_2 &= \underline{x}_2-\underline{x}_{2d}, \end{aligned} \tag{24}$$

where $\underline{x}_{1d}$ and $\underline{x}_{2d}$ are the desired vectors for tracking control of a quadrotor. The time derivatives of (24) is calculated as

$$\begin{aligned} \dot{\underline{s}}_1 &= \dot{\underline{x}}_1-\dot{\underline{x}}_{1d} = B_1(\underline{x}_1,\underline{x}_2)-\dot{\underline{x}}_{1d},\\ \dot{\underline{s}}_2 &= \dot{\underline{x}}_2-\dot{\underline{x}}_{2d} = \underline{f}_2(\underline{x}_1,\underline{x}_2)+B_2(\underline{x}_1,\underline{x}_2)\underline{u}-\dot{\underline{x}}_{2d}, \end{aligned}$$

$\underline{s}_1$ should converges to 0 to make quadrotor track the desired path thus set $\underline{x}_{2d}$ as follows:

$$\underline{x}_{2d} = B_1{}^+(\underline{x}_1)[dotunderx_{1d}+k\underline{s}_1-\rho_1 sgn(\underline{s}_1)],$$

where k and ρ_1 are positive contstants, and $B_1{}^+(\underline{x}_1)$ is the right pseudoinverse of $B_1(\underline{x}_1)$. $B_1{}^+(\underline{x}_1)$ always exists except $\theta=\pm\pi/2$ because $B_1(\underline{x}_1)$ has full rank. Likewise, set $\underline{u}$ to make $\underline{s}_2$ converge to 0 as follows [17-18]:

$$\begin{aligned} &\underline{u}=\\ &B_2{}^+(\underline{x}_1,\underline{x}_2)[\dot{\underline{x}}_{2d}-\underline{f}_2(\underline{x}_1,\underline{x}_2)-k\underline{s}_2-\rho_2 sgn(\underline{s}_2), \end{aligned} \tag{25}$$

where ρ_2 is a positive constant and $B_2^+(\underline{x}_1, \underline{x}_2)$ is the right pseudoinverse of $B_2(\underline{x}_1)$. $B_2^+(\underline{x}_1, \underline{x}_2)$ always exists because $B_2(\underline{x}_1, \underline{x}_2)$ has full rank. $\dot{\underline{x}}_{1d}$ and $\dot{\underline{x}}_{2d}$ are calculated as

$$\dot{\underline{x}}_{1d} = \frac{\underline{x}_{1d}(n) - \underline{x}_{1d}(n-1)}{\Delta t},$$
$$\dot{\underline{x}}_{2d} = \frac{\underline{x}_{2d}(n) - \underline{x}_{2d}(n-1)}{\Delta t},$$

where $\underline{x}_{1d}(n)$ and $\underline{x}_{2d}(n)$ are the nth calculated desired vectors and Δt is the sampling time. However, we cannot control all state variables of a quadrotor because a quadrotor is under-actuated system. Thus, the desired positions should be translated to the desired attitude angles for the tracking control of a quadrotor. For this, vectors are defined as follows:

$$\underline{a}_1 = (x, y, z),$$
$$\underline{a}_2 = (u, v, w),$$

For the tracking control of a quadrotor, the sliding surfaces are defined as follows:

$$\underline{s}_{1d} = \underline{a}_1 - \underline{a}_{1d},$$
$$\underline{s}_{2d} = \underline{a}_2 - \underline{a}_{2d}, \tag{26}$$

where $\underline{a}_{1d}$ and $\underline{a}_{2d}$ are the desired vectors of $\underline{a}_1$ and $\underline{a}_2$, respectively. The time derivatives of (26) is calculated as

$$\dot{\underline{s}}_{1d} = \dot{\underline{a}}_1 - \dot{\underline{a}}_{1d} = R\underline{a}_2 - \dot{\underline{a}}_{1d}$$
$$\dot{\underline{s}}_{2d} = \dot{\underline{a}}_2 - \dot{\underline{a}}_{2d}$$
$$= \begin{bmatrix} (vr - wq) + gS_\theta \\ (\wp - ur) - gC_\theta S_\phi \\ (uq - vp) - gC_\theta C_\phi + \dfrac{u_1}{m} \end{bmatrix} + \dot{\underline{a}}_{2d}$$

To make $\underline{s}_{1d}$ converge to 0, $\underline{a}_{2d}$ is set as follows:

$$\underline{a}_{2d} = R^{-1}[\dot{\underline{a}}_{1d} - k\underline{s}_{1d} - \rho_3 sgn(\underline{s}_{1d})],$$

where k_1 is a positive contstant larger than $1/2$ and ρ_3 is a positive constant. Likewise, to make $\underline{s}_{2d}$ converge to 0, define the virtual inputs as follows:

$$\begin{bmatrix} u_x \\ u_y \\ u_z \end{bmatrix} = \begin{bmatrix} -S_\theta \\ C_\theta S_\phi \\ C_\theta C_\phi \end{bmatrix} \tag{27}$$

Then, the virtual inputs are calculated to make $\underline{s}_{2d}$ converge to 0 as follows:

$$\begin{bmatrix} u_x \\ u_y \\ u_z \end{bmatrix} = \frac{1}{g}\left\{ \begin{bmatrix} (vr - wq) \\ (\wp - ur) \\ (uq - vp) + \dfrac{u_1}{m} \end{bmatrix} - \underline{a}_{2d} + k_1\underline{s}_{2d} + \rho_4 sgn(\underline{s}_{2d}) RIGHT \right.$$

where ρ_4 is a positive constant. The attitude angles ϕ and θ of a quadrotor can be calculated by (27) as

$$\theta = asin(-u_x),$$
$$\phi = asin\left(\frac{u_y}{C_{\theta d}}\right), \tag{28}$$

We can substitute the attitude angles into the desired angles in (28). Therefore, the desired angles can be calculated as follows:

$$\theta_d = asin(-u_x),$$
$$\phi_d = asin\left(\frac{u_y}{C_{\theta d}}\right), \tag{29}$$

If we substitute ϕ_d and θ_d in (24) into (29), a quadrotor tracks the desired path.

Theorem 2: A quadrotor asymptotically converges to the desired path if the designed control iputs (25) are applied to a quadrotor by setting k as follows:

$$k \geq \frac{1}{4} \| B_1(\underline{x}_1) \| \quad \| B_1(\underline{x}_1) \geq 4 \|, \qquad k \geq 1 \quad otherwise \tag{30}$$

Proof: We choose the Lyapunove function candidate as follows:

$$V_2 = \frac{1}{2}\underline{S}_1^T\underline{S}_1 + \frac{1}{2}\underline{S}_2^T\underline{S}_2 \tag{31}$$

The time derivative of (31) is calculated as

$$\begin{aligned}\dot{V}_2 &= \underline{s}_1^T\dot{\underline{s}}_1 + \underline{s}_2^T\dot{\underline{s}}_2 \\ &= -k\underline{s}_1^T\underline{s}_1 - \rho_1|\underline{s}_1| + \underline{s}_1^T B_1(\underline{x}_1)\underline{s}_2 \\ &\quad - k\underline{s}_2^T\underline{s}_2 - \rho_2|\underline{s}_2| \\ &= -k\underline{s}_1^T\underline{s}_1 - \rho_1|\underline{s}_1| - k\underline{s}_2^T\underline{s}_2 - \rho_2|\underline{s}_2| \\ &\quad + 2\underline{s}_1^T\frac{1}{2}B_1(\underline{x}_1)\underline{s}_2 \\ &\leq -k\underline{s}_1\end{aligned} \tag{32}$$

(32) will be negative definite if we set k as (30). The Lyapunov function candidate (31) is positive definite and the time derivative of candidate (32) is negative definite, thus the sliding surfaces $\underline{s}_1$ and $\underline{s}_2$ asymptotically converges to 0 by Lyapunov theorem. It means $\underline{x}_1$ asymptotically converges to $\underline{x}_{1d}$, thus a quadrotor asymptotically converges to the desired path.

When motor 1 of a quadrotor has fault during flight, the relation between the control inputs and the speed of each motor is described as follows:

$$\begin{aligned}u_1 &= b(ohm_2^2 + ohm_3^2 + ohm_4^2), \\ u_2 &= bl(ohm_4^2 - ohm_2^2), \\ u_3 &= blohm_3^2, \\ u_4 &= d(ohm_2^2 - ohm_3^2 + ohm_4^2),\end{aligned} \tag{33}$$

where ohm_2, ohm_3 and ohm_4 are unknown. Thus the solutions are not found because we have 4 equations and 3 unknowns. It means that we cannot control all of altitude, ϕ,θ, and ψ of a quadrotor. Thus we should sacrifice the controllability of ψ because the control of ψ is of little importance. Then, the relation between the control inputs and speed of each motor in fault case is described as follows:

$$\begin{bmatrix}u_1 \\ u_2 \\ u_3\end{bmatrix} = \begin{bmatrix} b & b & b \\ -bl & 0 & bl \\ 0 & bl & 0\end{bmatrix}\begin{bmatrix}ohm_{2f}^2 \\ ohm_{3f}^2 \\ ohm_{4f}^2\end{bmatrix} = F\begin{bmatrix}ohm_{2f}^2 \\ ohm_{3f}^2 \\ ohm_{4f}^2\end{bmatrix}, \tag{34}$$

where ohm_{2f}^2, ohm_{3f}^2 and ohm_{4f}^2 are the speed of each motor in fault case. Since constants b and l are not zero, F^{-1} always exists. Then, ohm_{2f}^2, ohm_{3f}^2 and ohm_{4f}^2 can be calculated as follows:

$$\begin{bmatrix}ohm_{2f}^2 \\ ohm_{3f}^2 \\ ohm_{4f}^2\end{bmatrix} = F^{-1}\begin{bmatrix}u_1 \\ u_2 \\ u_3\end{bmatrix} = \begin{bmatrix} b & b & b \\ -bl & 0 & bl \\ 0 & bl & 0\end{bmatrix}^{-1}\begin{bmatrix}u_1 \\ u_2 \\ u_3\end{bmatrix},$$

The fault tolerant control inputs of a quadrotor can be calculated as follows:

$$\begin{aligned}u_{1f} &= b(ohm_{2f}^2 + ohm_{3f}^2 + ohm_{4f}^2), \\ u_{2f} &= bl(ohm_{4f}^2 - ohm_{2f}^2), \\ u_{3f} &= blohm_{3f}^2, \\ u_{4f} &= d(ohm_{2f}^2 - ohm_{3f}^2 + ohm_{4f}^2),\end{aligned} \tag{35}$$

where u_{1f},u_{2f},u_{3f} and u_{4f} are the calculated fault tolerant control inputs of a quadrotor. We can

prove that a quadrotor asymptotically converges to the desired path if we apply the fault tolerant control inputs to a quadrotor after occurring the fault by Theorem 2.

IV. SIMULATIONS

In this section, we demonstrate the effectiveness and superiority of the proposed AFTC method. Without loss of generality, it is assumed that motor 1 of a quadrotor shown in Fig. 1 has the complete loss of effectiveness during flight. In the simulation for set to follow the continuous round path in the space. The equation of the path is as follows:

$$x_d = \begin{cases} 0 & (0 \le t \le 10) \\ 1-\cos\left(2\pi \times \dfrac{(t-10)}{40}\right) & (10 \le t \le 50) \end{cases}$$

$$y_d = \begin{cases} 0 & (0 \le t \le 10) \\ \sin\left(2\pi \times \dfrac{(t-10)}{40}\right) & (10 \le t \le 50) \end{cases}$$

$$z_d = \begin{cases} \dfrac{10}{t} & (0 \le t \le 50) \\ 1 & (0 \le t \le 50) \end{cases}$$

where, x_d, y_d and z_d is the object coordinate value over time on the earth-inertia frame.

The fault suddenly occurs on one motor at $t = 22s$ and the controller is switched to the designed fault tolerant controller after detecting the fault by the designed fault detection modules. In the simulation, we used the system parameter listed in Table. 1. To detect the fault, we also set the threshold values as follows:

$$\sigma_\phi = \sigma_\theta = 0.02$$

The simulation results are shown in Figs. 2 and 3. Figure 2 shows the results of tracking control for the fault on motor 1 without switching the controller to the designed fault tolerant controller. In this figure, the full line denotes the position of a quadrotor and the dashed line with circles denotes the desired path of a quadrotor. When the fault suddenly occurs on motor 1 at 22s, a quadrotor strays from the desired path and can no longer be controlled. However, a quadrotor tracks the desired path with small error after switching the controller

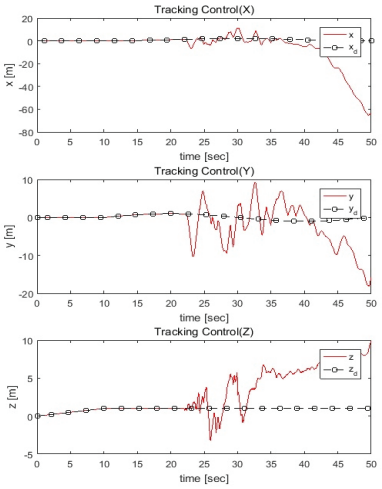

Fig. 2. The results of tracking control for the fault on motor 1 without switching the controller.

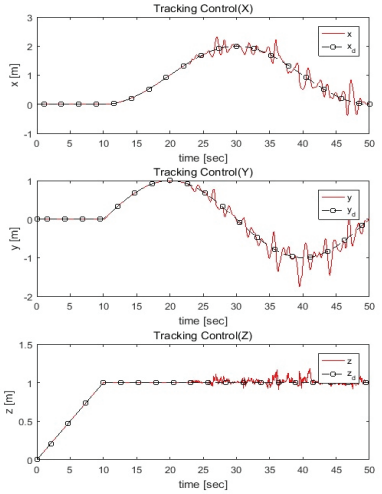

Fig. 3. The results of tracking control for the fault on motor 1 using the designed active fault tolerant controller.

Figure 3 shows the results of tracking control

for the fault of motor 1 with switching the controller to the designed fault tolerant controller. A quadrotor tracks the desired path well before the occurrence of the fault on motor 1. When the fault occurs on motor 1, a quadrotor strays from the desired path for a moment because of the time between the occurrence of a fault and the detection of a fault. It is 0.05s in the simulation. After detecting the fault, the controller is switched to the designed fault tolerant controller. The designed controller allows a quadrotor flies through the desired path with some error as shown in Fig. 3.

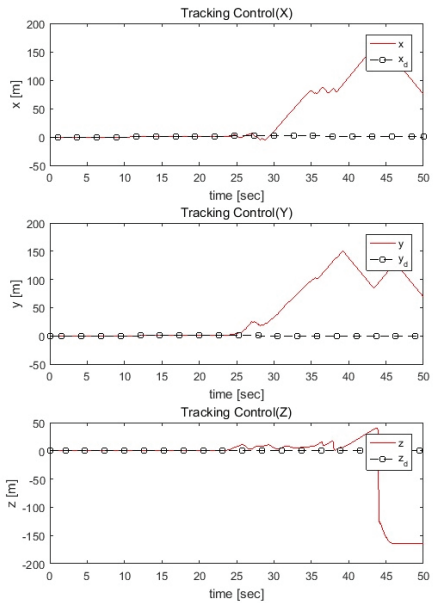

Fig. 4. The results of tracking control for the fault on motor 1 using the controller in [8].

To compare the performance of the fault tolerant controller, we test another fault tolerant controller designed in [8] in the simulation as shown in Fig. 4. Likewise, If a fault suddenly occurs on motor 1 at $t = 22s$, a quadrotor can not track the desired path anymore and consequently falls to the ground..

In this fiqure, the full line and the dashed line with circles denotes the position ans desired path of a quadrotor, respectively.

V. CONCLUSIONS

In this paper, we have proposed a method for designing an active fault tolerant controller for a quadrotor with complete loss of effectiveness of one motor. We derived the dynamics of a quadrotor using Lagrangian equation to represent the nonlinear quadrotor system. We designed the FDD and FDI modules using the nonlinear observer that observes the state variables of a quadrotor and formulated residual signals to detect the fault occurrence and the fault location. For the tracking control of a quadrotor after occurring the fault, we designed a fault tolerant controller for each motor, based on the MSSC method. Finally, we demonstrate the effectiveness of the designed FDD and FDI modules, and a fault tolerant controller via simulations results.

REFERENCES

[1] A. R. Merheb, F. Bateman, and H. Noura, "Design of passive fault-tolerant controllers of a quadrotor based on sliding mode theory," *Int. J. Appl. Math. Comput.* Sci., vol. 25, no. 3, Sept. 2015, pp. 561-576.

[2] T. Lombaerts, *Automatic flight control systems-Latest Developments.* Germany,–2012.

[3] A. R. Merheb, F. Bateman, and H. Noura, "Passive and active fault tolerant control of octorotor UAV using second order sliding mode control," *IEEE Conf. Control Appl.*, Sydney, Australia, 2015, pp. 1907-1912.

[4] T. Li, Y. Zhang, and B. W. Gordon, "Passive and active nonlinear fault-tolerant control of a quadrotor unmanned aerial vehicle based on the sliding mode control technique," *Proc. of Inst. Mech. Engineers Part I: J. Sys. Cotrol Engineering,* Vol. 227, No. 1, 2012, pp. 12-23.

[5] M. W. Mueller and R. D. Andrea, "Stability and control of a quadrocopter despite the complete loss of one, two, or three propellers," *Proc. of IEEE Int. Conf. Robot. Auto.*, Hongkong, China.

2014, pp. 45-52.
[6] M. W. Mueller and R. D. Andrea, "Relaxed hover solutions for multicopters: application to algorithmic redundancy and novel vehicles," *Proc. of Int. J. Robot. Research*, vol. 35, no. 8, Oct, 2015, pp. 873-889.
[7] S. Tashreef, L. Iftekhar, and S. A. Rahman, "Design of a crash-resistant PD-controlled quadcopter using coaxial propeller system," *Proc. of Int. Conf. Unmanned Aircraft Sys.*, Washington D.C, USA, 2016, pp. 986-992.
[8] R. C. Gomes and G. A. P. The, "PID-based fail-safe strategy against the break of opposite motors in quadcopters," *Proc. of Workshop on Research, Edu. Develop. Unmanned Aerial Sys.*, Cancon, Maxico, 2015, pp. 109-114.
[9] A. Chamseddine, D. Theilliol, Y. M. Zhang, C. John, and C. A. Rabbath, "Active fault-tolerant control system design with trajectory re-planning against actuator faults and saturation: Application to a quadrotor unmanned aerial vehicle," *Proc. of Int. J. Adapt. Control and Signal Process.*, vol. 29, no. 1, Nov. 2013, pp. 1-23.
[10] P. H. Zipfel, *Modeling and simulation of aerospace vehicle dynamics.* USA: Aiaa Education Series, 2007.
[11] L. R. G. Carrillo, A. E. D. Lopez, R. Lozano, and C. Pegard, *Quad rotorcraft control: vision based hovering and navigation.* Switzerland: Springer, 2012.
[12] T. Bresciani, "Modeling, identification and control of a quadrotor helicopter," Master's thesis, *Lund University*, 2008.
[13] R. W. Beard, "Quadrotor dynamics and control," Master's thesis, *Brigham Young University*, 2008.
[14] D. Mellinger, M. Shomin, and V. Kumar, "Control of quadrotors for robust perching and landing," *Proc. of the Int. Powered Lift Conf.*, Philadelphia, USA, 2010, pp. 205-225.
[15] A. R. Merheb, H. Noura, and F. Bateman, "Active fault tolerant control of quadrotor UAV using sliding mode control," *Proc. of Int. Conf. Unmanned Aircraft Sys.*, Orlando, USA, 2014, pp. 156-166.
[16] A. Freddi, "Model-based diagnosis and control of unmanned aerial vehicles: application to the quadrotor system," Ph. D's thesis, *Universita Politecnica Delle Marche*, 2012.
[17] Z. Lu, F. Lin, and H. Ying, "Multiple sliding surface control for systems in nonlinear block controllable form," *Cybernetics and Sys.: An Int. J.*, vol. 36, no. 5, Sept, 2006, pp. 513-526.
[18] J. K. Hedrick and P. P. Yip, "Multiple sliding surface control: theory and application," J. *Dynamic Sys. Measure. Control*, vol. 122, no. 4, pp. 586-593, December 2000.

저자 소개

Nam-Eung Hwang

He received the B.S. degree in school of electrical engineering in Inha University, Incheon, Korea in 2015. He received the M.S. degree in school of electrical and electronic engineering at Yonsei University, Seoul, Korea in 2017. He worked at ADD(Agency for Defence Development) as researcher until 2019 and at Duksan navcours Co. as associate researcher until 2021. Currently, he is working at Hanwha systems Co. as senior researcher.

His research interests nonlinear control, fault tolerant control, satellite navigation system, and MUMT(Manned-Unmanned Teaming)

Byung-Soo Kim

He received the B.S and M.S degrees in department of electronic engineering in Kyonggi University, Suwon, Korea in 2005 and 2007, respectively. Currently, he is in a Ph. D candidate in department of electronic engineering in Kyonggi University, Suwon, Korea and working to chief engineering for KET(Korea Electric Terminal)

His research interests intelligent control, robotics and control instrumentation.